

Response to the Editor of the manuscript

"Recent trends of groundwater temperatures in Austria"

by Benz et al. submitted to *Hydrology and Earth System Sciences*.

Manuscript Number: hess-2017-663

Revision due before: 15 May 2018

Editor comment:

The two reviews offer detailed points that require careful consideration and appropriate clarifications in a revised manuscript.

The authors' responses appear well thought out and convincing, and a revised manuscript reflecting the additional information and clarifications can fully address the reviews. Please proceed with a revision.

Reply: Thank you very much for editing our manuscript! In the following, please find the revised manuscript with marked changes.

Recent trends of groundwater temperatures in Austria

Susanne A. Benz¹, Peter Bayer², Gerfried Winkler³, Philipp Blum¹

¹Institute of Applied Geosciences (AGW), Karlsruhe Institute of Technology (KIT), Karlsruhe, 76131, Germany

²Institute of new Energy Systems (InES), Ingolstadt University of Applied Sciences, Ingolstadt, 85019, Germany

³Institute of Earth Sciences (IEW), NAWI Graz Geocenter, University of Graz, Graz, 8010, Austria

Correspondence to: Susanne Benz (susanne.benz@kit.edu)

Abstract

Climate change is one if not the most pressing challenge modern society faces. Increasing temperatures are observed all over the planet and the impact of climate change on the hydrogeological cycle has long been shown. However, so far we have insufficient knowledge on the influence of atmospheric warming on shallow groundwater temperatures. While some studies analyse the implication climate change has on selected wells, large scale studies are so far lacking. Here we focus on the combined impact of climate change in the atmosphere and local hydrogeological conditions on groundwater temperatures in 227 wells in Austria, which have in part been observed since 1964. A linear analysis finds a temperature change of $+ 0.7 \pm 0.8$ K in the years from 1994 to 2013. In the same timeframe surface air temperatures in Austria increased by 0.5 ± 0.3 K displaying a much smaller variety. However, most of the extreme changes in groundwater temperatures can be linked to local hydrogeological conditions. Correlation between groundwater temperatures and nearby surface air temperatures was additionally analysed. They vary greatly with correlation coefficients of -0.3 in central Linz to 0.8 outside of Graz. In contrast, the correlation of nationwide groundwater temperatures and surface air temperatures is high with a correlation coefficient of 0.83. All of these findings indicate that while atmospheric climate change can be observed in nationwide groundwater temperatures, individual wells are often primarily dominated by local hydrogeological conditions. In addition to the linear temperature trend, a step-wise model was also applied that identifies climate regime shifts, which were observed globally in the late 70s, 80s, and 90s. Hinting again at the influence of local conditions, at most 22 % of all wells show these climate regime shifts. However, we were able to identify an additional shift in 2007, which was observed by 37 % of all wells. Overall, the step-wise representation provides a slightly more accurate picture of observed temperatures than the linear trend.

1 Introduction

The thermal regime in the ground is coupled with the conditions in the atmosphere, and air temperature variations leave their traces in the ground. While, already at depth of a few meters, the amplitudes of periodic diurnal and seasonal temperature trends are strongly attenuated (Taylor and Stefan, 2009), long term non-periodic changes of air temperature permanently influence the subsurface down to greater depths of several tens to hundreds of meters (Beltrami et al., 2005). Worldwide, borehole temperature profiles therefore witness the increase of surface air temperature (SAT) due to recent climate (Huang et al., 2000; Harris and Chapman, 1997). In borehole climatology,

35 focus is set on “dry” boreholes in undisturbed natural areas, that is, boreholes with negligible influence of
36 groundwater flow and no direct human impacts. Borehole temperatures logged in such boreholes can be used to
37 invert vertical conductive heat transport models for deriving the corresponding trend of ground surface temperature
38 (GST). By assuming that GST and SAT are directly coupled or similar, past climate can be reconstructed. Many
39 boreholes, however, are located in urbanized areas and regions with past changes of land cover, where often
40 accelerated ground heat flux and higher GST are observed (Bense and Beltrami, 2007; Menberg et al., 2013; Bayer et
41 al., 2016; Cermak et al., 2017). Moreover, in humid climate regions boreholes are mostly not dry, but drilled for
42 groundwater use or monitoring. When dynamic groundwater flow conditions exist, then advective heat transport can
43 substantially affect the thermal regime in the subsurface (Ferguson et al., 2006; Kollet et al., 2009; Taylor and
44 Stefan, 2009; Stauffer et al., 2017; Westaway and Younger, 2016; Uchida et al., 2003). Additionally, recharge
45 processes, including snowmelt and rain-derived recharge, might impact the thermal regime of the shallow
46 subsurface. Previous studies, however, indicate that in many cases their influence can be neglected. Ferguson and
47 Woodbury (2005) and Bense and Kurylyk (2017) demonstrated that it is possible to estimate groundwater recharge
48 by using temperature-depth profiles based on the common assumption that the mean annual groundwater recharge
49 temperature is equal to the mean annual surface air temperature. Menberg et al. (2014) showed in their study that the
50 contribution of snowmelt-induced recharge with low temperature is minor in comparison to the overall recharge.
51 Finally, Molina-Giraldo et al. (2011) investigated the impact of seasonal temperature signals into an aquifer upon
52 bank infiltration including also varying groundwater recharge temperatures. They showed that the convective heat
53 transfer by groundwater recharge compared to conduction through the unsaturated zone and convection within the
54 aquifer is of minor impact. Still, the interplay of long-term climate variations, land use change and groundwater
55 produces a complex transient system, which is difficult if not impossible to accurately understand based on a few
56 borehole measurements (Irvine et al., 2016; Kupfersberger et al., 2017; Kurylyk et al., 2017; Kurylyk et al., 2014;
57 Kurylyk et al., 2013; Taniguchi and Uemura, 2005; Taniguchi et al., 1999; Zhu et al., 2015).

58 The consequence of climate change on aquifers was illuminated with respect to groundwater recharge and
59 availability of freshwater resources (Moeck et al., 2016; Scibek and Allen, 2006; Holman, 2006; Gunawardhana and
60 Kazama, 2011; Loáiciga, 2003), groundwater quality impacts (Kolb et al., 2017) and effects on groundwater (-
61 dependent) ecosystems (Burns et al., 2017; Jyväskylä et al., 2015; Kløve et al., 2014; Andrushchyshyn et al., 2009;
62 Hunt et al., 2013). Taylor et al. (2012) summarized various connections and feedbacks between climate change and
63 groundwater. A key parameter is the temperature, which is expected to increase in shallow groundwater globally
64 following with some delay following roughly the trends in the atmosphere. However, long-term measurements of
65 temperature evolution in groundwater are rare (Watts et al., 2015; Figura et al., 2015). Instead often well
66 measurements taken at a few different time points are compared to indicate elevated temperatures, such as by
67 Gunawardhana and Kazama (2011) for the Sendai Plain in Japan, by Šafanda et al. (2007) for boreholes in the Czech
68 Republic, Slovenia and Portugal, and Yamano et al. (2009) and Menberg et al. (2013) for urban areas in Eastern Asia
69 and Central Europe. Others, such as Kupfersberger (2009) and Menberg et al. (2014) examine repeated temperature
70 records of single or a few selected wells. The work by Lee et al. (2014) is one of the very few studies on long term
71 groundwater temperature (GWT) time series recorded for a larger area. They applied linear regression to hourly
72 temperature data recorded from 2000 to 2010 at 78 South Korean national groundwater monitoring sites. They found

73 a mean increase of 0.1006 K/year and concluded that shallow ground and surface temperature show moderate
74 proportionality. Lee et al. (2014), however, reported that 12 wells revealed decreasing GWT trends without further
75 details on potential factors. Blaschke et al. (2011) applied trend analyses on long term data sets of mean annual GWT
76 of 112 and 255 wells for the time periods 1955-2006 and 1976-2006 respectively in Austria. They found increasing
77 trends of the GWT in shallow porous aquifers related to increasing air temperature. Similar insights from other
78 regions are lacking still, and the contribution of atmospheric warming to long-term GWT evolution is nearly
79 unexplored.

80 In the presented study, GWTs of 227 wells in Austria, **measured in part since 1966**, are analysed and regional
81 patterns and temperature anomalies are identified. In contrast to Blaschke et al. (2011) focus here is not only set on
82 linear trends, but also on detection of climate regime shifts in the measured GWT, following the suggestions by
83 Figura et al. (2011) and Menberg et al. (2014). As a relevant mode of global climate variability, long-lived decadal
84 patterns such as the Atlantic or Pacific decadal oscillation have been identified, **e.g. Minobe (1997) and Rodionov**
85 **(2004). These control atmospheric temperatures as well and are often described as sudden, step-wise temperature**
86 **changes separating stable periods, called climate regimes.** Even if these regime shifts arrive attenuated and delayed
87 in shallow groundwater, they can be detected and thus can offer another hint on the influence of climatic variations.
88 Aside from the statistical analysis of GWT time series, the influence of land cover as well as their correlation to
89 surface air temperature is investigated to scrutinize potential local influences on the measured data.

90 **2 Material and Methods**

91 **2.1 Material**

92 **Geology, Hydrogeology and Climate of Austria**

93 The Austrian Alps as the main part of the European Eastern Alps are characterized by a complex geology with
94 various lithologies and have been built up during multiple tectonic phases striking now in a West-East direction. The
95 complexity of the tectonic and geologic settings of the European Alps and in particular of the European Eastern Alps
96 is described and discussed by numerous authors (e.g. Schmid et al., 2004; Linzer et al., 2002). Active tectonic
97 evolution resulting in high topography and uplift rates coincide largely with high stream power (Robl et al., 2017;
98 Robl et al., 2008) and thus, have an impact on the drainage system of the Alps. During the Pleistocene the Alps were
99 affected by glaciations with a strong impact on the morphology in particular on the inner alpine valleys and the
100 foreland. Due to sedimentation during the Holocene these areas now contain quaternary porous aquifers. The herein
101 analysed wells are located in shallow aquifers representing these quaternary sediments in the inner alpine valleys and
102 foreland basin. Based on a compiled geology a hydrogeological overview as a hydrogeological map of Austria is
103 provided by Schubert et al. (2003).

104 Climate and climate trends during the last two century (1800-2000) of the Great Alpine Region (European Alps and
105 their surrounding foreland, GAR) was intensively investigated during last decades yielding in the HISTALP data set
106 (Auer et al., 2007). This data set left its mark on the regional classification of climate zones by Köppen-Geiger where
107 Austria is mainly divided into three climate zones, warm temperate, boreal, and alpine.

108 **Groundwater Temperatures**

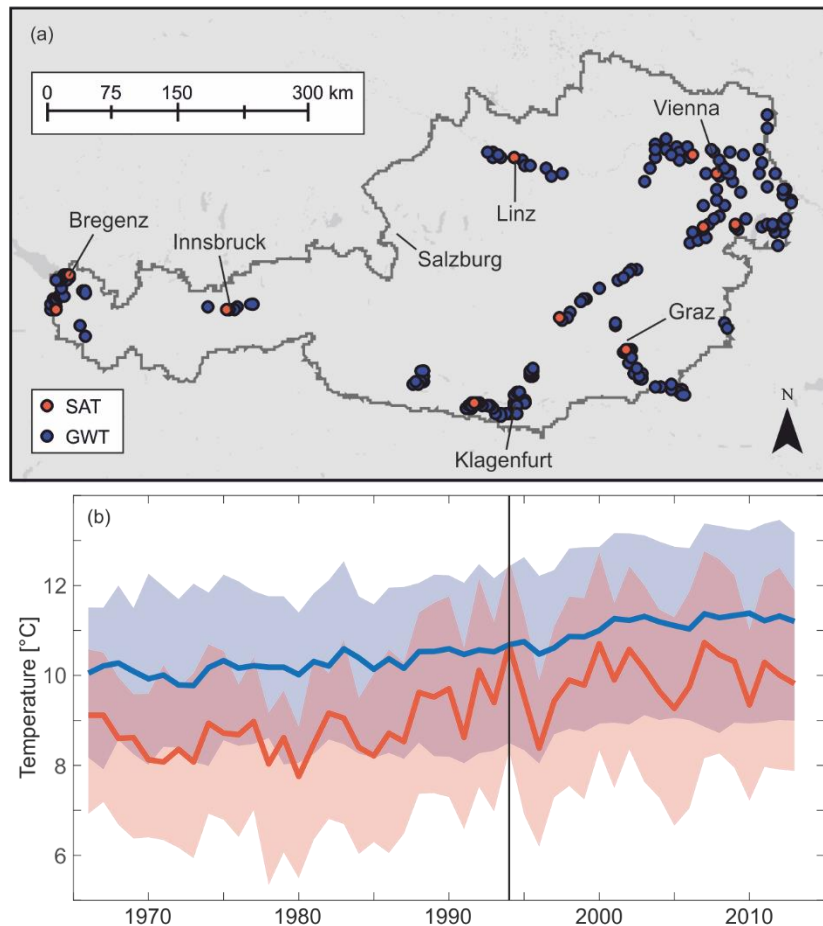
109 In Austria, GWTs up to Dec 2013 are provided by the Austrian Federal Ministry of Sustainability and Tourism
110 Directorate-General IV. - Water Management (BMNT, former Federal Ministry of Agriculture, Forestry,
111 Environment and Water Management (BMLFUW) in 1138 wells. Here, we focus on all wells with a measurement
112 depth of less than 30 m, a record of at least 20 years and no major breaks (> 3 month) in the last 20 years of the time
113 series. Hence, all studied wells are monitored at least since Jan 1994, and some already since 1966 (see Fig. S1a for
114 more information). Additionally wells impacted by geothermal hot springs were excluded. Overall, in this study
115 annual mean data of 227 individual wells from all over the country (Fig. 1a) are analysed. Years with less than 9
116 months of data are excluded. For the timeframe 1994 and 2013, this amounts to 74 excluded data points in 60 wells.
117 Additionally, only 9-11 months of data were available for 260 data points in 122 wells. To minimize the associated
118 bias, these small gaps in the time series were filled using a linear fit. Hence small errors for years without a full set of
119 monthly mean data have to be expected.

120 The average measurement depth in the wells is 7 ± 4 m below ground surface (Fig. S1b). All wells are located in the
121 Cfb climate zone of the Köppen-Geiger classification, warm temperate climate with warm summers and no dry
122 seasons (Rubel et al., 2017). The spatial median GWTs and inner 90 % percentiles for all wells are displayed in Fig.
123 1b. The obtained temperature in Fig. 1b increases from around 9.8 °C in 1966 to 11.4 °C in 2013.

124 Following the CORINE Land Cover (CLC) data from 2012 (Fig. S2a), 45 % of all wells are under artificial surfaces,
125 46 % under agricultural areas, and 9 % under forest following the $100 \text{ m} \times 100 \text{ m}$ classification. In addition, CLC
126 from 1990 was consulted, however, no land cover changes near any of the analysed wells are observed. Overall, for
127 the time period 1994 – 2013, absolute GWTs of the monitored wells under artificial surfaces are on average 1.5 ± 0.3
128 K warmer than GWTs under forest; GWTs under agricultural areas are on average 0.6 ± 0.2 K warmer than GWTs
129 under forest (Fig. S2b). This validates previous findings by Benz et al. (2017b) for GWTs in Germany, who
130 identified even larger differences of up to 3 K between the individual land cover classes.

131 **Surface Air Temperatures**

132 Surface air temperatures (SATs) within Austria are monitored by the Central Institution for Meteorology and
133 Geodynamics (ZAMG), Austria. In this study data from 12 individual weather stations are being analysed, each one
134 is located within 5 km of at least one analysed well and in the same climate zone (Cfb). Their location is displayed in
135 Fig. 1a. Again annual mean data was available for a time period of 1966 to 2013 (Fig. 1b). As expected and as
136 previously shown in Benz et al. (2017b) for SAT and Benz et al. (2017a) for land surface temperatures, above
137 ground temperatures are generally lower than GWTs. All 12 analysed weather stations are located in areas classified
138 as artificial surface and experienced no land cover changes.



139

140 **Figure 1. (a) Location of all analysed groundwater temperature (GWT - 227 wells) and surface air**
 141 **temperature (SAT - 12 weather stations) measurement points; (b) temporal evolution of the spatial median,**
 142 **annual mean temperatures for groundwater (blue) and air (red). The inner 90 percentiles are marked in**
 143 **lighter colours. All time series were monitored since at least 1994.** 2.2 Method

144 **Correlations**

145 Within this study, the Spearman correlation coefficient was determined, as it is especially robust to outliers caused
 146 for example by heat waves, which impact air temperatures but have only minor effect on groundwater temperatures.
 147 When determining the correlation between two time series, missing years were ignored. Next to the correlation
 148 between GWT and SAT, correlation between all individual wells and weather stations were determined in order to
 149 create a plot similar to a (semi)variogram that shows the correlation between two measurement stations depending on
 150 their distance to each other.

151 **Linear analysis**

152 Equivalent to the work by Lee et al. (2014), a linear temperature change was determined for all 227 wells. For this, a
 153 linear regression model of the annual mean temperature data was determined in Matlab 2016b. Because all wells in
 154 our dataset were continuously monitored between 1994 and 2013, only this timeframe was analysed.

155 **Climate regime shifts**

156 Climate data is often thought to not change linearly, but in form of a step function, dividing a time series into
157 individual climate regimes of a constant mean (Andrushchyshyn et al., 2009; Minobe, 1997). These regimes are
158 changed when so-called climate regime shifts (CRS) occur and long-term mean values change. While several
159 methods to model these shifts have been in use (Easterling and Peterson, 1995), in recent years the method by
160 Rodionov (2004) became standard. It identifies the significance of each possible shift by calculating the so-called
161 Regime Shift Index (RSI): the cumulative sum of the normalized differences between the observed values and the
162 long term mean of the assumed regime. Only shifts with a positive RSI are considered significant, and a higher value
163 of RSI denotes a more pronounced CRS. The entire algorithm is described in detail by Rodionov (2004). This
164 sequential analysis is data driven and requires no prior knowledge of the timing of possible shifts. It was updated to
165 further include prewhitening in order to reduce background noise (Rodionov, 2006) and is available online as a
166 Microsoft Excel add-in (NOAA). In this study we applied the method to the complete time series of all 227 wells and
167 12 weather stations. Because the algorithm cannot handle gaps within the analysed series, gaps in our data were
168 filled using a linear fit. All parameters were set to the same values as in the work by Menberg et al. (2014), who
169 applied the method to four GWT time series in Germany. A target significance level of 0.15 was used by Menberg et
170 al. and in our analysis, the cut off length was set to 10 years and the Huber weight parameter was set to 1.

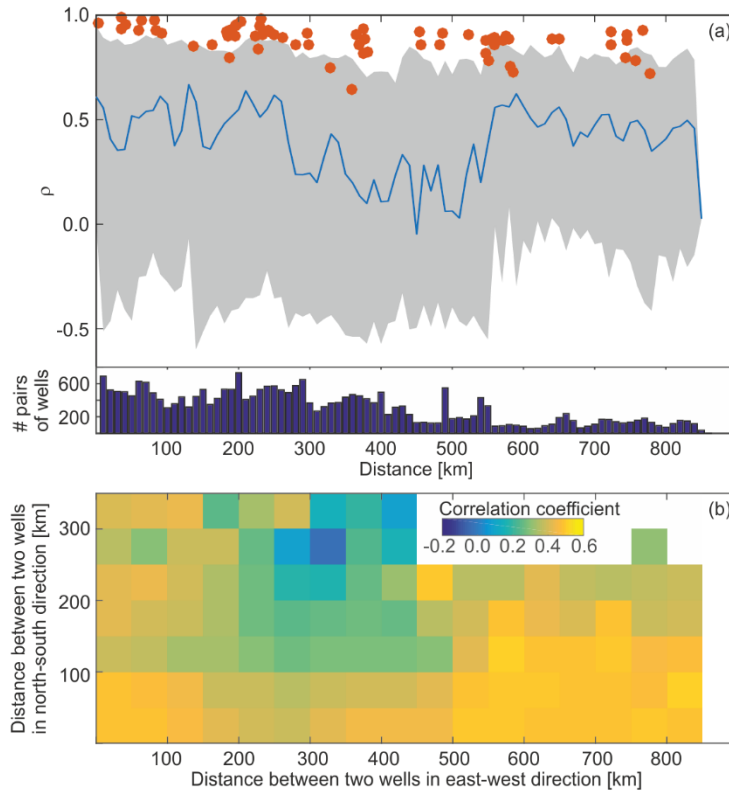
171 **3 Results and Discussion**

172 **3.1 Correlations**

173 Figure 2a displays the correlation between different wells or rather different weather stations in relation to their
174 distance to each other. Shown is the distance between two wells/weather stations on the x-axis and the corresponding
175 spearman correlation coefficient between them. For the weather station, each individual pair is shown by a red point,
176 for GWTs, as there are many possible pairs of wells, the line gives the moving median (± 25 km) correlation of all
177 pairs at the corresponding distances. The inner 90 percentiles are shown in grey, and correlation coefficients close to
178 or below zero are determined for several pairs of wells. However, here p-values are generally also close to one and
179 GWTs do not correlate. This is most likely due to local heat sources impacting at least on well in these pairs.

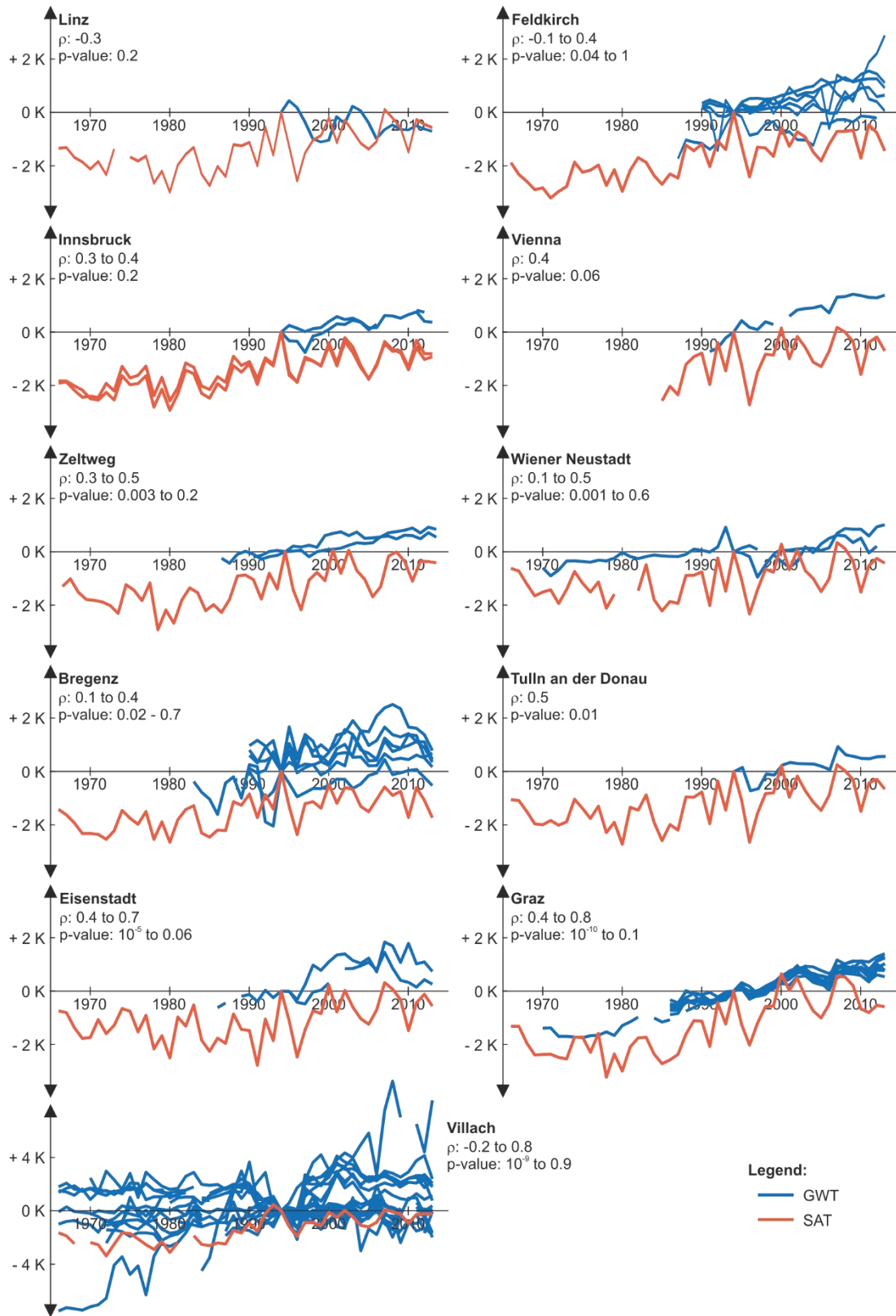
180 As expected the moving average correlation decreases with distance. This decrease is more extreme in GWTs than in
181 SATs and GWTs correlate less than SATs overall. This agrees with the observations in Benz et al. (2017b), who
182 showed that annual mean GWTs show greater variations than SAT over the same distances.

183 Additionally, the correlation between two wells seems to be anisotropic: correlation coefficients between two wells
184 decrease faster with north-south distance than with west-east distance (Fig. 2b), which can be explained by the
185 dominant striking direction of the geology and the resulting topography in Austria, where valleys generally run from
186 west to east. Hence, larger rivers typically follow this direction and wells at the same latitude experience similar
187 temperature signals.



188

189 **Figure 2. Influence of distance on the correlation between the annual means of two measurement points. a) Correlation**
 190 **between SAT time series is given in red, median correlation between GWT time series is given in blue. The inner 90**
 191 **percentile are coloured in grey, the number of pairs of wells per distance is shown in dark blue below.** b) The colour gives
 192 **the median correlation between GWTs of two wells in relation to their absolute distance to each other in east-west**
 193 **direction (x-axis) and in north-south direction (y-axis).**



194

195 **Figure 3. Change from 1994 in surface air temperature (SAT) and groundwater temperatures (GWTs) of all wells within**
196 **5 km of the analysed weather station. See Fig. S3 for an overview of the locations. Minimum and maximum correlations**
197 **and p-values between individual wells and weather stations are given.**

198 In a next step, correlations between GWT and SAT are determined. On a country-wide scale Spearman correlation
199 coefficient between spatial median GWT and SAT (Fig. 1b) is 0.83. In comparison correlation between individual
200 weather stations and wells are shown in Fig. 3, locations are displayed in detail in Fig. S3. Here correlations vary
201 greatly and Spearman correlation coefficients are < 0.5 for about half of all wells within 5 km of a weather station.
202 This indicates that GWTs are often influenced by local causes and not necessarily solely by local SATs. The lowest
203 correlation is determined in Linz where the groundwater is intensively used for cooling and heating (Krakow and
204 Fuchs-Hanusch, 2016). The studied well is located within the city centre next to train tracks and office buildings.
205 Hence, it is very likely that the thermal properties of the groundwater are dominated by anthropogenic influences
206 from heated buildings and underground structures as often the case in subsurface urban heat islands (Menberg et al.,
207 2013, 2013; Benz et al., 2015; Benz et al., 2016; Attard et al., 2016). This would also explain the high GWTs that are
208 on average 3.3 K warmer than the local annual mean SAT. Like the well, the weather station is also located within
209 the city centre.

210 The best correlations between individual pairs of a well and a weather station can be observed in the southern part of
211 the city of Graz, where all wells and the weather station are located close to or within the Graz airport, respectively.
212 The well with the highest correlation of 0.80 to SAT is located less than 1 km from the weather station close to the
213 airport parking lot next to suburban housing. It is continuously monitored since 1970 and the longest time series in
214 the area. The well with the lowest correlation (0.45) to the weather station here is located slightly to the east near a
215 dog-park and suburban housing. Here observations started in 1994, it is the shortest time series in this area. At all
216 other wells, measurements began in 1986 and show correlations between 0.6 and 0.7 to SAT indicating that the
217 duration of the measurements play a significant role for local comparisons. In contrast, duration of the time series
218 appears to be of minor importance on a countrywide scale. For example, the long time series in Wiener Neustadt
219 (Fig. 3), which started measurements in 1970 and is located near a mineral extraction site, has a correlation of 0.48
220 and is therefore comparable to the short time series in Graz, starting in 1994 located in a suburban area.

221 Additionally, measurement depths of GWT can have an impact on the correlation between SAT and GWT. While it
222 is generally assumed that a measurement depth closer to the surface results in a better correlation with SAT as there
223 is less of a shift between both datasets, this is only the case for some of the here analysed locations such as Villach
224 (Figure S4a). In contrast, correlation increases with GWT measurement depth for other locations such as the one in
225 Graz. This might be related to local underground heat sources such as sewage systems impacting GWT near the
226 surface more than temperatures at greater depth. However, as the depth of the wells analysed here varies only
227 slightly, no definite conclusions can be drawn without further inspection of specific cases.

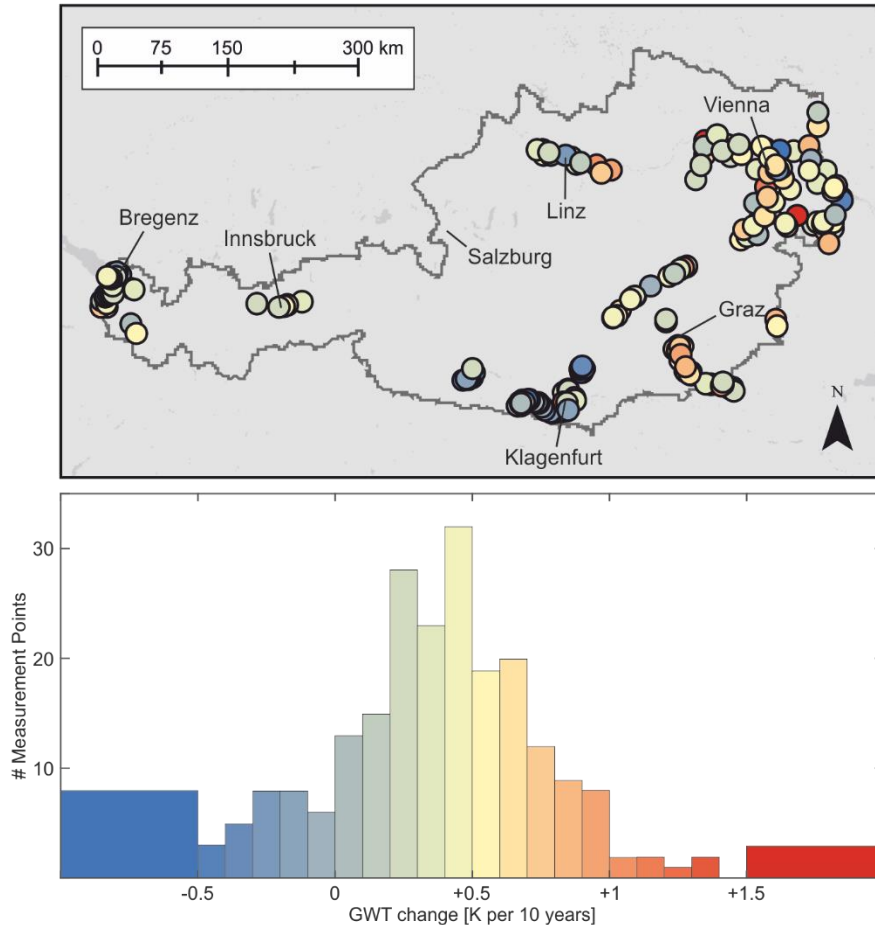
228 **Table 1. Correlation coefficient and corresponding p-value between spatial median SAT and spatial median GWT for all**
 229 **analysed SAT locations, and additional information.**

Location	Number of wells	Measurement depth GWT [m below surface]	Number of weather stations	Spearman correlation	p-value	Population ¹
Linz	1	10	1	-0.31	10 ⁻¹	192,000
Feldkirch	6	4 to 17	1	0.19	10 ⁻¹	31,000
Innsbruck	2	10	2	0.37	10 ⁻¹	123,000
Vienna	1	12	1	0.41	10 ⁻²	1,740,000
Zeltweg	2	6 to 7	1	0.48	10 ⁻³	7,000
Wiener Neustadt	2	9 to 20	1	0.51	10 ⁻⁴	42,000
Bregenz	6	4 to 10	1	0.52	10 ⁻³	28,000
Tulln an der Donau	1	7	1	0.54	10 ⁻²	15,000
Eisenstadt	2	4 to 5	1	0.67	10 ⁻⁴	13,000
Graz	9	4 to 12	1	0.73	10 ⁻⁸	266,000
Villach	17	3 to 11	1	0.80	10 ⁻¹¹	60,000

230 ¹ Register-based Labour Market Statistics 2014, municipality level (Statistik Austria).

231 Table 1 displays the correlations between spatial median GWT and spatial median SAT for each of the SAT
 232 locations in Figs. 3 and S3. For all locations with at least two wells besides Zeltweg and Graz correlation does
 233 improve when spatial median GWT is analysed instead of the individual locations. In all likelihood the spatial
 234 median GWT provides a more general temperature trend that is not influenced by local influences on temperatures
 235 such as construction work, plant development and shading, and is therefore more closely related to surface air
 236 temperatures.

237 In addition, the data indicates that city size or rather population of the city does not necessarily influence the
 238 correlation between GWT and SAT (Table 1). For example, both locations Graz (population of more than 250,000)
 239 and Eisenstadt (population of 13,000) have similar correlation coefficients despite their different population.
 240 Meanwhile, Bregenz and Feldkirch have a similar population (~30,000) and number of wells (six), but different
 241 correlation coefficients (0.52 and 0.19). However, it is also important to note that not all wells analysed here are
 242 located in the city centre, still all of them are within close proximity (< 250 m) of anthropogenically used areas (Fig.
 243 S3).



244
 245 **Figure 4. Increase in temperature for all individual measurement points for the 20-year timeframe 01/1994 to 12/2013. The**
 246 **mean change in groundwater temperature is $+0.4 \pm 0.5$ K per 10 years.**

247 **3.2 Linear temperature change**

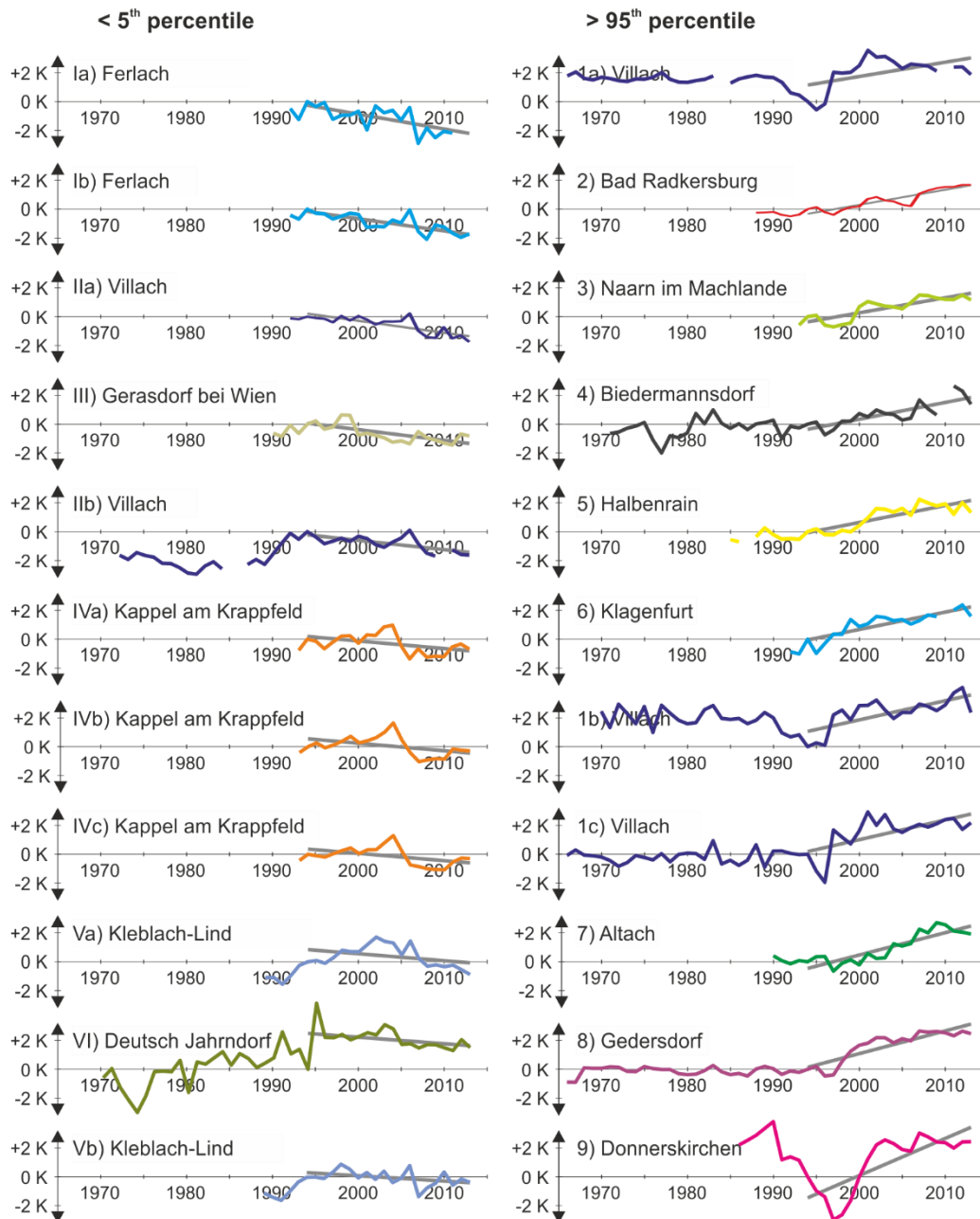
248 **During the time between 1994 and 2013, GWTs have changed on average by $+0.36 \pm 0.44$ K per 10 years and SAT**
 249 **on average by $+0.24 \pm 0.13$ K per 10 years. The lower changes in SAT are most likely due to the chosen timeframe:**
 250 **A heat wave in summer 1994 led to extraordinary high annual mean SAT in this year (Figure 1b) and thus impacts**
 251 **the determined linear temperature change.** The increase of GWT is in good agreement with results of a former study
 252 considering data sets of Austria from 1976-2006 (Blaschke et al., 2011). However, it is more than double the global
 253 air temperature increase determined by Jones et al. (1999) for the timeframe 1978 to 1997 with $+0.32$ K in 20 years
 254 and less than the numbers given in the work by Ji et al. (2014). In their global study they give an air temperature
 255 increase of more than 0.4 K for the timeframe 2000 to 2009 for the northern mid-latitudes including Austria. Fig. 4
 256 displays a map and a histogram of all determined GWT changes. **There appears to be no significant influence of land**
 257 **cover on the observed temperature change (Fig. S2c). Median temperature change is approximately 0.4 ± 0.4 K per**
 258 **10 years for groundwater under artificial surfaces and forest areas, and 0.3 ± 0.5 K per 10 years under cultivated**
 259 **areas. However, temperature change decreases slightly with GWT measurement depth by approximately 0.015 K per**
 260 **10 years per meter (Fig. S4b). This relationship can be related to deeper temperatures corresponding to earlier**
 261 **temperatures, when temperature increase was less severe. However, because the vast majority of temperatures are**

262 monitored at a depth of less than 15 m and show a high variability in linear temperature change, this number must be
263 taken with caution. R^2 of the fit is only 0.02 and RMSE is 0.4 K.

264 To evaluate the goodness of this linear approach when representing climate change, RMSE of the fit was determined
265 for each well for 1994 to 2013. We found an average RMSE of 0.4 ± 0.2 °C.

266 When looking at the individual wells, no obvious spatial pattern for temperature changes is visible (Fig. 4). However,
267 most wells with temperature changes lower than the 5th percentile are located close to the river Drava in Ferlach,
268 Villach, and Kleblach-Lind in the very South of Austria (Fig. 5 and Fig. S5). Although, they are up to 80 km away
269 from each other, all of these wells show a sudden drop in temperatures in the year 2007 (wells Ia, Ib, IIa, IIb, Va, and
270 Vb marked blue in Fig. 5). This temperature reduction can be seen in most of the 27 wells that are less than 1 km
271 from the Drava away (Fig. S6), for 24 of these wells, temperatures in 2006 are more than 0.6 K warmer than
272 temperatures in 2008. However, temperatures (as well as additional parameters such as water level) within the river
273 do not indicate any connection between this sudden temperature reduction and the Drava river (Fig. S6). Either way,
274 further research is necessary to identify the cause of this temperature anomaly.

275 Additionally, three other wells in the lowest 5 percent of temperature change are all located less than 10 km from
276 each other near the village Kappel am Krappfeld (wells IVa, b and c marked orange in Fig. 5). They and also
277 additional surrounding wells show a steep decline in temperatures in 2006 before temperatures start to increase
278 steadily again. These wells seem to be affected by the new drinking water supply (four wells with a total pumping
279 rate of about 100 l/s) located about 1 km in the south. This demonstrates the importance of including groundwater
280 flow when trying to interpret groundwater temperature. In general, most of the extreme changes in temperature
281 appear to be linked to local causes and do not happen gradually, but rather rapidly over the short time span of one or
282 two years. Another example of this can be seen in wells with temperature changes higher than the 95th percentile
283 (Fig. 5 and Fig. S7). While these highest five percentiles of all wells do not show local clusters to the same extent as
284 the lowest 5 percentiles and can be observed all over the country, three wells (1a, 1b and 1c, marked dark blue in Fig.
285 5) are located in the industrial area of Villach in the South of Austria. Here some construction work during 1997 is
286 likely the cause of the sudden temperature increase but concrete evidence could not be identified.



287

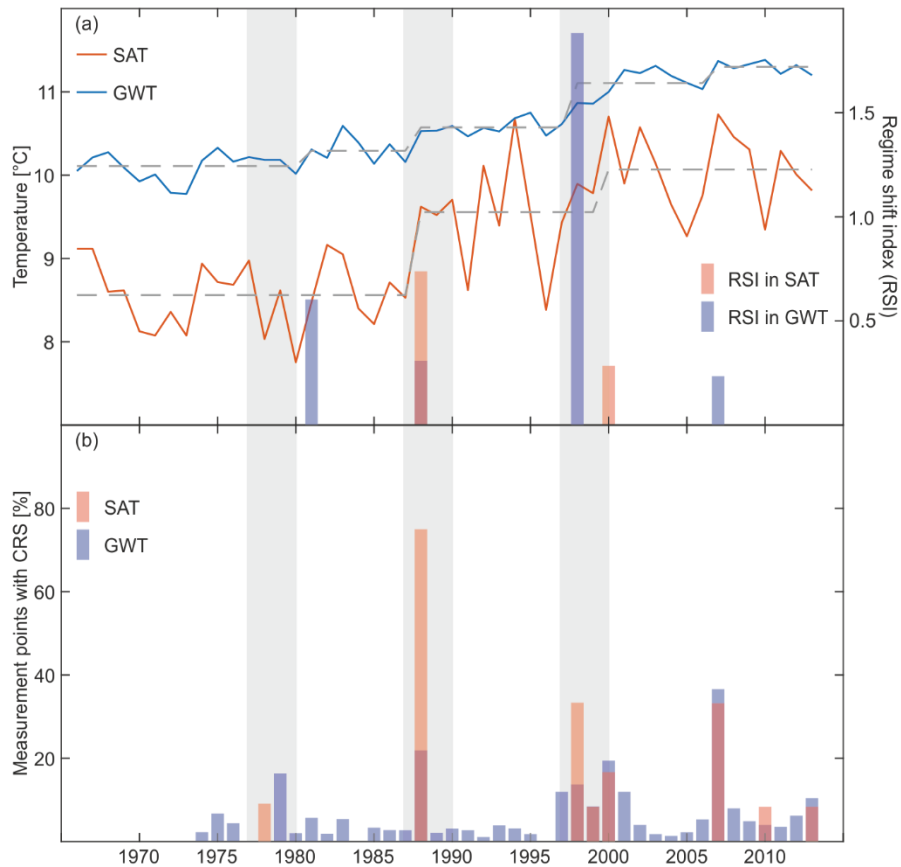
288 **Figure 5. Annual mean time series and linear fit (in grey) of the wells with the lowest (left side, numbered with roman**
 289 **numbers) and highest (right side, numbered with arabic numbers) temperature changes in the time frame 1994 and 2013.**
 290 **See Fig. S5 and S7 for an overview of the locations. They are placed in ascending orders with the highest temperature**
 291 **change at the bottom.**

292 3.3 Climate regime shifts

293 All detected climate regime shifts (CRS) of **the spatial median temperatures** time series are shown in Fig. 6a. Overall
 294 GWTs increase by 1.2 K between the first and last CRS and SAT increased by 1.5 K.

295 Global climate regime shifts (CRS) in air and also groundwater were detected for the late 70s, the late 80s and the
 296 late 90s by Menberg et al. (2014). Using the same algorithm spatial median annual mean GWT and SAT in Austria
 297 show shifts in the late 80s and 90s (Fig. 6a). GWTs show additional shifts in 1981 and 2007. While the shift in the

298 late 80s is observed during the same year (1988) in GWT and SAT, the shift in the late 90s appears earlier and is
 299 more significant in GWTs. However, because SATs are the drivers of GWTs and not vice versa, the fact that the
 300 GWT change precedes the SAT change suggests that this method does not have the necessary resolution to determine
 301 short time lags between SATs and GWTs. Accordingly the detected time shifts in wells within 5 km of a weather
 302 station do generally not indicate the same CRS as the weather station: Of 56 CRS observed in at least one well only
 303 12 are also observed in a nearby weather station no more than one year before (Fig. S8). However, it is also
 304 important to note that some of the analysed time series only span over a 20 year time period and are thus on the
 305 shorter end for a statistically relevant analysis of climate regime shifts (Rodionov, 2006).



306
 307 **Figure 6. (a) Median groundwater temperature (blue) and surface air temperature (red) of all wells or rather weather**
 308 **stations as well as the corresponding climate regime shifts (CRS) in form of the regime shift index (RSI). (b) Percentage of**
 309 **measurement points in GWT (blue) and SAT (red) that show a CRS in each year. The analysis of global temperatures data**
 310 **indicates a regime shift at the end of the 70s, the 80s and the 90s which are shown here in as grey bars.**

311 Like with the linear approach, the goodness of the CRS and corresponding statistical step model was evaluated by
 312 determining the RMSE for the time period 1994 to 2013. We determined a mean RMSE value of 0.3 ± 0.1 K, which
 313 is slightly better than the RMSE for the linear fit as determined above (0.4 ± 0.2 K). Only 20 of the 227 analysed
 314 wells have a better RMSE with the linear approach than the statistical step model of the CRS approach. Hence, we
 315 conclude that the CRS method is slightly more appropriate to simulate temperature changes in groundwater than a
 316 linear approach even for time periods as short as 20 years. However, when the individual wells and weather stations
 317 are analysed (Fig. 6b), globally observed CRS can be identified in at most 22 % (1988) of all wells. Results further
 318 show that the shift in the 90s is temporally more spread out than the shifts in the 70s and 80s in both GWT and SAT.

319 This indicates that this shift is less well defined and temperatures of the globe became more variable in their
320 temporal evolution. In accordance to this interpretation there is a higher percentage wells with a CRS in all years
321 after 1996 than before. Furthermore, more than one third of all weather stations and wells detect a shift in 2007
322 indicating this year as the start of a new climate regime within Austria. While a CRS in 2007 was not observed by
323 Menberg et al. (2014) whom studied earlier time series than here, this year was also identified by Litzow and Mueter
324 (2014) as the start of a new regime for both climate and biological indicators within the North Pacific Ocean.
325 However the dimension of the shifts do not always agree for all wells. For example, wells experiencing a shift
326 observed in 2007 include all wells along the Drau observed in Fig. 5 and S5, which show a sudden drop in
327 temperature for this year. In contrast, the countrywide time series in Fig. 6a indicates a positive shift in temperatures.

328 **4 Conclusions**

329 Temperatures in 227 shallow wells and 12 weather stations in Austria, monitored in part since 1966, were analysed
330 in this study. Linear temperature change was determined and revealed a general increase in temperature between the
331 years 1994 and 2013 of approximately $+0.36 \pm 0.44$ K per 10 years in the groundwater and on average $+0.24 \pm 0.13$
332 K per 10 years in the air. Most extreme changes in groundwater temperatures, especially temperature decrease, could
333 be linked to local causes such as the **installation** of a new drinking water supply that influences nearby groundwater
334 wells. **This reveals the extent in which groundwater temperatures are dominated by local events, groundwater flow,**
335 **and the thermal properties of the surrounding. When solving local problems we can therefore not recommend relying**
336 **on average relationships valid on a nation scale.** Accordingly correlation between annual mean groundwater
337 temperatures and nearby (< 5 km) air temperatures varies greatly from -0.3 in Linz to 0.8 near Graz. However, if
338 spatial median groundwater temperatures and surface air temperatures of all of Austria are compared, we found a
339 significant correlation of 0.83 demonstrating once more that groundwater temperatures are closely linked to surface
340 temperatures and therefore experience climate change. However, globally observed climate regime shifts in the late
341 70s, 80s and 90s could only be identified in approximately 20 % of all wells. Nevertheless, we were able to observe
342 another shift in 2007 in 37% of all wells and 33 % of all weather stations indicating this year as the possible start of a
343 new climate regime within the alpine region. **However, further research dedicated to other climate parameters such**
344 **as permafrost and snowfall is necessary to validate these findings. Additionally, our observations made in Austria**
345 **should be transferred to similar regions in the world testing the transferability of the presented results.** Overall
346 climate regimes represent measured temperature slightly better (RMSE: 0.3 ± 0.1 K) than the linear fit (RMSE: $0.4 \pm$
347 0.2 K).

348 **Acknowledgements**

349 We would like to thank Erich Fischer (BMNT, former BMLFUW) for information and data regarding groundwater
350 temperatures and Alexander Orlik (ZAMG) for information and data regarding surface air temperatures of Austria.

351 Furthermore, we would like to acknowledge the financial support for the first author by the portfolio project
352 “Geoenergy” of the Helmholtz Association of German Research Centres (HGF) and the support by Deutsche

353 Forschungsgemeinschaft and Open Access Publishing Fund of Karlsruhe Institute of Technology. A big thank you
354 also to one anonymous reviewer and to R. Hunt for their helpful and very constructive comments.

355 **References**

356 Andrushchyn, O. P., Wilson, K. P., and Williams, D. D.: Climate change-predicted shifts in the temperature
357 regime of shallow groundwater produce rapid responses in ciliate communities, *Global Change Biol*, 15, 2518–
358 2538, doi:10.1111/j.1365-2486.2009.01911.x, 2009.

359 Attard, G., Rossier, Y., Winiarski, T., and Eisenlohr, L.: Deterministic modeling of the impact of underground
360 structures on urban groundwater temperature, *The Science of the total environment*, 572, 986–994,
361 doi:10.1016/j.scitotenv.2016.07.229, 2016.

362 Auer, I., Böhm, R., Jurkovic, A., Lipa, W., Orlik, A., Potzmann, R., Schöner, W., Ungersböck, M., Matulla, C.,
363 Briffa, K., Jones, P., Efthymiadis, D., Brunetti, M., Nanni, T., Maugeri, M., Mercalli, L., Mestre, O., Moisselin,
364 J.-M., Begert, M., Müller-Westermeier, G., Kveton, V., Bochnicek, O., Stastny, P., Lapin, M., Szalai, S.,
365 Szentimrey, T., Cegnar, T., Dolinar, M., Gajic-Capka, M., Zaninovic, K., Majstorovic, Z., and Nieplova, E.:
366 HISTALP—historical instrumental climatological surface time series of the Greater Alpine Region, *Int. J.*
367 *Climatol*, 27, 17–46, doi:10.1002/joc.1377, 2007.

368 Bayer, P., Rivera, J. A., Schweizer, D., Schärli, U., Blum, P., and Rybach, L.: Extracting past atmospheric warming
369 and urban heating effects from borehole temperature profiles, *Geothermics*, 64, 289–299,
370 doi:10.1016/j.geothermics.2016.06.011, 2016.

371 Beltrami, H., Ferguson, G., and Harris, R. N.: Long-term tracking of climate change by underground temperatures,
372 *Geophysical Research Letters*, 32, 1–4, 2005.

373 Bense, V. and Beltrami, H.: Impact of horizontal groundwater flow and localized deforestation on the development
374 of shallow temperature anomalies, *J. Geophys. Res.*, 112, 327, doi:10.1029/2006JF000703, 2007.

375 Bense, V. F. and Kurylyk, B. L.: Tracking the Subsurface Signal of Decadal Climate Warming to Quantify Vertical
376 Groundwater Flow Rates, *Geophys. Res. Lett.*, 44, 12,244-12,253, doi:10.1002/2017GL076015, 2017.

377 Benz, S. A., Bayer, P., and Blum, P.: Global patterns of shallow groundwater temperatures, *Environ. Res. Lett.*, 12,
378 34005, doi:10.1088/1748-9326/aa5fb0, 2017a.

379 Benz, S. A., Bayer, P., and Blum, P.: Identifying anthropogenic anomalies in air, surface and groundwater
380 temperatures in Germany, *The Science of the total environment*, 584-585, 145–153,
381 doi:10.1016/j.scitotenv.2017.01.139, 2017b.

382 Benz, S. A., Bayer, P., Goettsche, F. M., Olesen, F. S., and Blum, P.: Linking Surface Urban Heat Islands with
383 Groundwater Temperatures, *Environmental science & technology*, 50, 70–78, doi:10.1021/acs.est.5b03672,
384 2016.

385 Benz, S. A., Bayer, P., Menberg, K., Jung, S., and Blum, P.: Spatial resolution of anthropogenic heat fluxes into
386 urban aquifers, *The Science of the total environment*, 524-525, 427–439, doi:10.1016/j.scitotenv.2015.04.003,
387 2015.

388 Blaschke, A. P., Merz, R., Parajka, J., Salinas, J., and Blöschl, G.: Auswirkungen des Klimawandels auf das
389 Wasserdargebot von Grund- und Oberflächenwasser, *Österr Wasser- und Abfallw*, 63, 31–41,
390 doi:10.1007/s00506-010-0273-3, 2011.

391 BMNT: Austrian Federal Ministry of Sustainability and Tourism Directorate-General IV. - Water Management,
392 eHYD, <http://ehyd.gv.at/>.

393 Burns, E. R., Zhu, Y., Zhan, H., Manga, M., Williams, C. F., Ingebritsen, S. E., and Dunham, J. B.: Thermal effect of
394 climate change on groundwater-fed ecosystems, *Water Resour. Res.*, 53, 3341–3351,
395 doi:10.1002/2016WR020007, 2017.

396 Cermak, V., Bodri, L., Kresl, M., Dědeček, P., and Šafanda, J.: Eleven years of ground-air temperature tracking over
397 different land cover types, *Int. J. Climatol*, 37, 1084–1099, doi:10.1002/joc.4764, 2017.

398 Easterling, D. R. and Peterson, T. C.: A new method for detecting undocumented discontinuities in climatological
399 time series, *Int. J. Climatol*, 15, 369–377, doi:10.1002/joc.3370150403, 1995.

400 Ferguson, G., Beltrami, H., and Woodbury, A. D.: Perturbation of ground surface temperature reconstructions by
401 groundwater flow?, *Geophys. Res. Lett.*, 33, 951, doi:10.1029/2006GL026634, 2006.

402 Ferguson, G. and Woodbury, A. D.: The effects of climatic variability on estimates of recharge from temperature
403 profiles, *Ground Water*, 43, 837–842, doi:10.1111/j.1745-6584.2005.00088.x, 2005.

404 Figura, S., Livingstone, D. M., Hoehn, E., and Kipfer, R.: Regime shift in groundwater temperature triggered by the
405 Arctic Oscillation, *Geophys. Res. Lett.*, 38, n/a-n/a, doi:10.1029/2011GL049749, 2011.

406 Figura, S., Livingstone, D. M., and Kipfer, R.: Forecasting Groundwater Temperature with Linear Regression
407 Models Using Historical Data, *Ground Water*, 53, 943–954, doi:10.1111/gwat.12289, 2015.

408 Gunawardhana, L. N. and Kazama, S.: Climate change impacts on groundwater temperature change in the Sendai
409 plain, Japan, *Hydrol. Process.*, 25, 2665–2678, doi:10.1002/hyp.8008, 2011.

410 Harris, R. N. and Chapman, D. S.: Borehole Temperatures and a Baseline for 20th-Century Global Warming
411 Estimates, *Science*, 275, 1618–1621, doi:10.1126/science.275.5306.1618, 1997.

412 Holman, I. P.: Climate change impacts on groundwater recharge- uncertainty, shortcomings, and the way forward?,
413 *Hydrogeol J*, 14, 637–647, doi:10.1007/s10040-005-0467-0, 2006.

414 Huang, S., Pollack, H. N., and Shen, P. Y.: Temperature trends over the past five centuries reconstructed from
415 borehole temperatures, *Nature*, 403, 756–758, 2000.

416 Hunt, R. J., Walker, J. F., Selbig, W. R., Westenbroek, S.M., and Regan, R. S.: Simulation of Climate-Change
417 Effects on Streamflow, Lake Water Budgets, and Stream Temperature Using GSFLOW and SNTMP, Trout
418 Lake Watershed, Wisconsin, Scientific-Investigations Report, 2013-5159, 118 p., 2013.

419 Irvine, D. J., Cartwright, I., Post, V. E.A., Simmons, C. T., and Banks, E. W.: Uncertainties in vertical groundwater
420 fluxes from 1-D steady state heat transport analyses caused by heterogeneity, multidimensional flow, and climate
421 change, *Water Resour. Res.*, 52, 813–826, doi:10.1002/2015WR017702, 2016.

422 Ji, F., Wu, Z., Huang, J., and Chassignet, E. P.: Evolution of land surface air temperature trend, *Nature Climate
423 change*, 4, 462–466, doi:10.1038/nclimate2223, 2014.

424 Jones, P. D., New, M., Parker, D. E., Martin, S., and Rigor, I. G.: Surface air temperature and its changes over the
425 past 150 years, *Rev. Geophys.*, 37, 173–199, doi:10.1029/1999RG900002, 1999.

426 Jyväsjärvi, J., Marttila, H., Rossi, P. M., Ala-Aho, P., Olofsson, B., Nisell, J., Backman, B., Ilmonen, J., Virtanen, R.,
427 Paasivirta, L., Britschgi, R., Kløve, B., and Muotka, T.: Climate-induced warming imposes a threat to north
428 European spring ecosystems, *Global Change Biol*, 21, 4561–4569, doi:10.1111/gcb.13067, 2015.

429 Kløve, B., Ala-Aho, P., Bertrand, G., Gurdak, J. J., Kupfersberger, H., Kværner, J., Muotka, T., Mykrä, H., Preda,
430 E., Rossi, P., Uvo, C. B., Velasco, E., and Pulido-Velazquez, M.: Climate change impacts on groundwater and
431 dependent ecosystems, *Journal of Hydrology*, 518, 250–266, doi:10.1016/j.jhydrol.2013.06.037, 2014.

432 Kolb, C., Pozzi, M., Samaras, C., and VanBriesen, J. M.: Climate Change Impacts on Bromide, Trihalomethane
433 Formation, and Health Risks at Coastal Groundwater Utilities, *ASCE-ASME J. Risk Uncertainty Eng. Syst., Part
434 A: Civ. Eng.*, 3, 4017006, doi:10.1061/AJRUA6.0000904, 2017.

435 Kollet, S. J., Cvijanovic, I., Schüttemeyer, D., Maxwell, R. M., Moene, A. F., and Bayer, P.: The Influence of Rain
436 Sensible Heat and Subsurface Energy Transport on the Energy Balance at the Land Surface, *Vadose Zone
437 Journal*, 8, 846, doi:10.2136/vzj2009.0005, 2009.

438 Krakow, S. and Fuchs-Hanusch, D.: Fernkälteversorgung zur Vermeidung von Grundwassererwärmungen und
439 Nutzungskonflikten am Beispiel der Stadt Linz – Bewertung auf Basis ÖWAV-Regelblatt 207 und qualitativer
440 Nutzwertanalyse, *Österr Wasser- und Abfallw*, 68, 354–367, doi:10.1007/s00506-016-0324-5, 2016.

441 Kupfersberger, H.: Heat transfer modelling of the Leibnitzer Feld aquifer, Austria, *Environ Earth Sci*, 59, 561–571,
442 doi:10.1007/s12665-009-0054-0, 2009.

443 Kupfersberger, H., Rock, G., and Draxler, J. C.: Inferring near surface soil temperature time series from different
444 land uses to quantify the variation of heat fluxes into a shallow aquifer in Austria, *Journal of Hydrology*, 552,
445 564–577, doi:10.1016/j.jhydrol.2017.07.030, 2017.

446 Kurylyk, B. L., Bourque, C. P.-A., and MacQuarrie, K. T. B.: Potential surface temperature and shallow groundwater
447 temperature response to climate change: An example from a small forested catchment in east-central New
448 Brunswick (Canada), *Hydrol. Earth Syst. Sci.*, 17, 2701–2716, doi:10.5194/hess-17-2701-2013, 2013.

449 Kurylyk, B. L., Irvine, D. J., Carey, S. K., Briggs, M. A., Werkema, D. D., and Bonham, M.: Heat as a groundwater
450 tracer in shallow and deep heterogeneous media: Analytical solution, spreadsheet tool, and field applications,
451 *Hydrol. Process.*, 31, 2648–2661, doi:10.1002/hyp.11216, 2017.

452 Kurylyk, B. L., MacQuarrie, K. T.B., and McKenzie, J. M.: Climate change impacts on groundwater and soil
453 temperatures in cold and temperate regions: Implications, mathematical theory, and emerging simulation tools,
454 *Earth-Science Reviews*, 138, 313–334, doi:10.1016/j.earscirev.2014.06.006, 2014.

455 Lee, B., Hamm, S.-Y., Jang, S., Cheong, J.-Y., and Kim, G.-B.: Relationship between groundwater and climate
456 change in South Korea, *Geosci J*, 18, 209–218, doi:10.1007/s12303-013-0062-7, 2014.

457 Linzer, H.-G., Decker, K., Peresson, H., Dell'Mour, R., and Frisch, W.: Balancing lateral orogenic float of the
458 Eastern Alps, *Tectonophysics*, 354, 211–237, doi:10.1016/S0040-1951(02)00337-2, 2002.

459 Litzow, M. A. and Mueter, F. J.: Assessing the ecological importance of climate regime shifts: An approach from the
460 North Pacific Ocean, *Progress in Oceanography*, 120, 110–119, doi:10.1016/j.pocean.2013.08.003, 2014.

461 Loáiciga, H. A.: Climate Change and Ground Water, *Annals of the Association of American Geographers*, 93, 30–
462 41, doi:10.1111/1467-8306.93103, 2003.

463 Menberg, K., Blum, P., Kurylyk, B. L., and Bayer, P.: Observed groundwater temperature response to recent climate
464 change, *Hydrol. Earth Syst. Sci.*, 18, 4453–4466, doi:10.5194/hess-18-4453-2014, 2014.

465 Menberg, K., Blum, P., Schaffitel, A., and Bayer, P.: Long-term evolution of anthropogenic heat fluxes into a
466 subsurface urban heat island, *Environmental science & technology*, 47, 9747–9755, doi:10.1021/es401546u,
467 2013.

468 Minobe, S.: A 50-70 year climatic oscillation over the North Pacific and North America, *Geophys. Res. Lett.*, 24,
469 683–686, doi:10.1029/97GL00504, 1997.

470 Moeck, C., Brunner, P., and Hunkeler, D.: The influence of model structure on groundwater recharge rates in
471 climate-change impact studies, *Hydrogeol J*, 24, 1171–1184, doi:10.1007/s10040-016-1367-1, 2016.

472 Molina-Giraldo, N., Bayer, P., Blum, P., and Cirpka, O. A.: Propagation of seasonal temperature signals into an
473 aquifer upon bank infiltration, *Ground Water*, 49, 491–502, doi:10.1111/j.1745-6584.2010.00745.x, 2011.

474 NOAA: Regime Shift Detection, <http://www.beringclimate.noaa.gov/regimes/>.

475 Robl, J., Heberer, B., Prasicek, G., Neubauer, F., and Hergarten, S.: The topography of a continental indenter: The
476 interplay between crustal deformation, erosion, and base level changes in the eastern Southern Alps, *J. Geophys.*
477 *Res. Earth Surf.*, 122, 310–334, doi:10.1002/2016JF003884, 2017.

478 Robl, J., Hergarten, S., and Stüwe, K.: Morphological analysis of the drainage system in the Eastern Alps,
479 *Tectonophysics*, 460, 263–277, doi:10.1016/j.tecto.2008.08.024, 2008.

480 Rodionov, S. N.: A sequential algorithm for testing climate regime shifts, *Geophys. Res. Lett.*, 31, n/a-n/a,
481 doi:10.1029/2004GL019448, 2004.

482 Rodionov, S. N.: Use of prewhitening in climate regime shift detection, *Geophys. Res. Lett.*, 33, 336,
483 doi:10.1029/2006GL025904, 2006.

484 Rubel, F., Brugger, K., Haslinger, K., and Auer, I.: The climate of the European Alps: Shift of very high resolution
485 Köppen-Geiger climate zones 1800–2100, *metz*, 26, 115–125, doi:10.1127/metz/2016/0816, 2017.

486 Šafanda, J., Rajver, D., Correia, A., and Dědeček, P.: Repeated temperature logs from Czech, Slovenian and
487 Portuguese borehole climate observatories, *Clim. Past*, 3, 453–462, doi:10.5194/cp-3-453-2007, 2007.

488 Schmid, S. M., Fgenschuh, B., Kissling, E., and Schuster, R.: Tectonic map and overall architecture of the Alpine
489 orogen, *Eclogae geol. Helv.*, 97, 93–117, doi:10.1007/s00015-004-1113-x, 2004.

490 Schubert, G., Bayer, I., Lampl, H., Shadlau, S., Wurm, M., Pavlik, W., Pestal, G., Rupp, C., and Schild, A.:
491 Hydrogeologische Karte von Österreich 1: 500.000, Verlag der Geologischen Bundesanstalt, 2003.

492 Scibek, J. and Allen, D. M.: Modeled impacts of predicted climate change on recharge and groundwater levels,
493 *Water Resour. Res.*, 42, 270, doi:10.1029/2005WR004742, 2006.

494 Statistik Austria: Bevölkerungsstand,
495 http://www.statistik.at/web_de/statistiken/menschen_und_gesellschaft/bevoelkerung/volkszaehlungen_registerzaehlungen_abgestimmte_erwerbsstatistik/bevoelkerungsstand/index.html.
496

497 Stauffer, F., Bayer, P., Blum, P., Giraldo, N. M., and Kinzelbach, W.: Thermal use of shallow groundwater, CRC
498 Press, [S.l.], 2017.

499 Taniguchi, M., Shimada, J., Tanaka, T., Kayane, I., Sakura, Y., Shimano, Y., Dapaah-Siakwan, S., and Kawashima,
500 S.: Disturbances of temperature-depth profiles due to surface climate change and subsurface water flow: 1. An
501 effect of linear increase in surface temperature caused by global warming and urbanization in the Tokyo
502 Metropolitan Area, Japan, *Water Resour. Res.*, 35, 1507–1517, doi:10.1029/1999WR900009, 1999.

503 Taniguchi, M. and Uemura, T.: Effects of urbanization and groundwater flow on the subsurface temperature in
504 Osaka, Japan, *Physics of the Earth and Planetary Interiors*, 152, 305–313, doi:10.1016/j.pepi.2005.04.006, 2005.

505 Taylor, C. A. and Stefan, H. G.: Shallow groundwater temperature response to climate change and urbanization,
506 *Journal of Hydrology*, 375, 601–612, doi:10.1016/j.jhydrol.2009.07.009, 2009.

507 Taylor, R. G., Scanlon, B., Döll, P., Rodell, M., van Beek, R., Wada, Y., Longuevergne, L., Leblanc, M., Famiglietti,
508 J. S., Edmunds, M., Konikow, L., Green, T. R., Chen, J., Taniguchi, M., Bierkens, M. F. P., MacDonald, A.,
509 Fan, Y., Maxwell, R. M., Yechieli, Y., Gurdak, J. J., Allen, D. M., Shamsudduha, M., Hiscock, K., Yeh, P. J.-F.,
510 Holman, I., and Treidel, H.: Ground water and climate change, *Nature Climate change*, 3, 322–329,
511 doi:10.1038/nclimate1744, 2012.

512 Uchida, Y., Sakura, Y., and Taniguchi, M.: Shallow subsurface thermal regimes in major plains in Japan with
513 reference to recent surface warming, *Physics and Chemistry of the Earth, Parts A/B/C*, 28, 457–466,
514 doi:10.1016/S1474-7065(03)00065-2, 2003.

515 Watts, G., Battarbee, R. W., Bloomfield, J. P., Crossman, J., Daccache, A., Durance, I., Elliott, J. A., Garner, G.,
516 Hannaford, J., Hannah, D. M., Hess, T., Jackson, C. R., Kay, A. L., Kernan, M., Knox, J., Mackay, J., Monteith,
517 D. T., Ormerod, S. J., Rance, J., Stuart, M. E., Wade, A. J., Wade, S. D., Weatherhead, K., Whitehead, P. G., and
518 Wilby, R. L.: Climate change and water in the UK – past changes and future prospects, *Progress in Physical*
519 *Geography*, 39, 6–28, doi:10.1177/0309133314542957, 2015.

520 Westaway, R. and Younger, P. L.: Unravelling the relative contributions of climate change and ground disturbance to
521 subsurface temperature perturbations: Case studies from Tyneside, UK, *Geothermics*, 64, 490–515,
522 doi:10.1016/j.geothermics.2016.06.009, 2016.

523 Yamano, M., Goto, S., Miyakoshi, A., Hamamoto, H., Lubis, R. F., Monyrath, V., and Taniguchi, M.:
524 Reconstruction of the thermal environment evolution in urban areas from underground temperature distribution,
525 *The Science of the total environment*, 407, 3120–3128, doi:10.1016/j.scitotenv.2008.11.019, 2009.

526 Zhu, K., Bayer, P., Grathwohl, P., and Blum, P.: Groundwater temperature evolution in the subsurface urban heat
527 island of Cologne, Germany, *Hydrol. Process.*, 29, 965–978, doi:10.1002/hyp.10209, 2015.

528